

EFFECT OF VISCOPLASTIC FLOW RULES ON THE INITIATION AND GROWTH OF SHEAR BANDS AT HIGH STRAIN RATES

R. C. BATRA and C. H. KIM

Department of Mechanical and Aerospace Engineering and Engineering Mechanics,
University of Missouri-Rolla, Rolla, MO 65401-0249, U.S.A.

(Received 3 July 1989; in revised form 30 October 1989)

ABSTRACT

MARCHAND and Duffy have reported detailed measurements of the temperature and strain as a shear band develops in a HY-100 steel. Assuming their torsional tests in thin-wall tubes can be adequately modeled by a viscoplastic block undergoing overall adiabatic simple shearing deformations, we investigate the effect of modeling the viscoplastic response of the material by a power law, and flow rules proposed by Litonski, Bodner and Partom, and Johnson and Cook. Each of these flow rules is first calibrated by using the test data at a nominal strain-rate of 3300 s^{-1} . Then predictions from the use of these flow rules at nominal strain-rates of 1400 s^{-1} and 1600 s^{-1} are compared with the experimental findings. It is found that the Bodner–Partom law and the dipolar theory proposed by Wright and Batra predict reasonably well the main features of the shear band formation in a HY-100 steel.

1. INTRODUCTION

THE DEVELOPMENT of shear bands in metals undergoing plastic deformations at high strain-rates usually precedes shear fractures. For this and other reasons their study has received considerable attention during the last ten years. ROGERS (1983) and TIMOTHY (1987) have surveyed various aspects of shear banding. BAI (1981), CLIFTON (1980) and BURNS (1985) among others have investigated conditions which will lead to the growth or decay of perturbations superimposed on a viscoplastic body deformed homogeneously in simple shear. MOLINARI and CLIFTON (1987), TZAVARAS (1987) and WRIGHT (1990) have studied the problem in greater detail. For rigid/perfectly plastic materials, WRIGHT (1990) has developed a criterion that ranks materials according to their tendency to form adiabatic shear bands.

The numerical study of shear banding has been conducted, among others, by SHAWKI *et al.* (1983), WRIGHT and BATRA (1985), BATRA (1987), BATRA and KIM (1990), ANAND *et al.* (1988), NEEDLEMAN (1989), LEMONDS and NEEDLEMAN (1986a, 1986b), and BATRA and LIU (1989). These works have employed different viscoplastic flow rules and have examined, qualitatively, different aspects of shear banding in simple shearing and plane-strain compression problems. A material inhomogeneity or defect has been simulated by either introducing a temperature perturbation or assuming the existence of weak material at the site of the defect.

Most of the earlier experimental work (e.g. ZENER and HOLLOMON, 1944; MOSS, 1981; COSTIN *et al.*, 1980) has reported observations made after the shear band had formed. Recently HARTLEY *et al.* (1987), GIOVANOLA (1987), and MARCHAND and DUFFY (1988) have given histories of the temperature and strain within a band as it develops. This facilitates a detailed comparison of the numerical and experimental results undertaken here. We presume that the torsional experiments of MARCHAND and DUFFY (1988) on thin-wall steel tubes can be analysed by studying the thermomechanical deformations of a viscoplastic block undergoing overall adiabatic simple shearing deformations. We consider four different flow rules, namely the power law (e.g. see SHAWKI *et al.*, 1983), and those due to LITONSKI (1977), BODNER and PARTOM (1975), and JOHNSON and COOK (1983). Also, because of the presence of steep strain gradients near the edges of the shear band, we consider the effect of including strain gradients and the corresponding dipolar stresses in the analysis. We note that WRIGHT and BATRA (1987), COLEMAN and HODGDON (1985), and ZBIB and AIFANTIS (1988) have considered the effect of strain gradients in their works. DILLON and KRATOCHVIL (1970) motivated the consideration of strain gradients and dipolar stresses as one way to account for the interaction among dislocations.

The computed results show that the dipolar theory predicts, quantitatively, various experimentally observed features of shear banding very well. The Bodner–Partom law for nonpolar materials also predicts well the initial growth of the shear band. Other flow rules fail to predict, in a noticeable way, one or more aspects of experimental results. This should not be taken as the final word for these viscoplastic laws since our calibration technique used to find values of various material parameters involves solving a nonlinear coupled thermomechanical initial-boundary-value problem and we may get the same stress–strain curve for different combinations of the values of material parameters. Nevertheless, the computed results do favor exploring further refinements of the dipolar theory and the Bodner–Partom law.

2. FORMULATION OF THE PROBLEM

A realistic modeling of MARCHAND and DUFFY's (1988) experiments on the twisting of thin-wall tubes requires analysing three-dimensional thermomechanical dynamic deformations of a viscoplastic body. Postponing this ultimate goal and striving to find the most appropriate viscoplastic flow rule, we study here dynamic thermomechanical deformations of a viscoplastic block undergoing overall adiabatic simple shearing deformations. In terms of non-dimensional variables, the governing equations can be written as (e.g. see BATRA, 1987)

$$\rho \dot{v} = (s - l\sigma_{,y})_{,y}, \quad 0 < y < 1, \quad (2.1)$$

$$\dot{\theta} = k\theta_{,yy} + s\dot{\gamma}_p + l\sigma\dot{d}_p, \quad 0 < y < 1, \quad (2.2)$$

$$\dot{s} = \mu(v_{,y} - \dot{\gamma}_p), \quad (2.3)$$

$$\dot{\sigma} = \mu l(v_{,yy} - \dot{d}_p), \quad (2.4)$$

$$\dot{\gamma}_p = g(s, \sigma, \gamma_p, d_p, \theta, l), \quad (2.5)$$

$$\dot{d}_p = lh(s, \sigma, \dot{\gamma}_p, d_p, \theta, l). \quad (2.6)$$

These equations, written for dipolar materials, reduce to those for nonpolar materials when l is set equal to zero. Here ρ is the mass density, v is the velocity of a material particle in the direction of shearing, a superimposed dot indicates the material time derivative, s is the shearing stress, l a material characteristic length, σ the dipolar stress, and a comma followed by y signifies partial differentiation with respect to y . Furthermore, k is the thermal conductivity, $\dot{\gamma}_p$ is the plastic strain-rate, \dot{d}_p the dipolar plastic strain-rate, μ the shear modulus, and θ is the temperature change from that in the reference configuration. Whereas (2.1) expresses the balance of linear momentum and (2.2) the balance of internal energy, (2.3)–(2.6) are constitutive relations. The different viscoplastic flow rules differ in the functional forms of g and h and are discussed below in the next section.

For the initial conditions we take

$$\begin{aligned} v(y, 0) = 0, s(y, 0) = 0, \sigma(y, 0) = 0, \\ \theta(y, 0) = \varepsilon(1 - y^2)^9 e^{-5y^2}. \end{aligned} \quad (2.7)$$

That is, in the initial rest state of the block, it is taken to be stress free. The initial temperature distribution simulates the defect or inhomogeneity in the block assumed to be present near the point $y = 0$; the value of ε represents the strength of the defect.

We presume that the overall deformations of the block are adiabatic and the lower surface is at rest while the upper surface is assigned a velocity that increases linearly from 0 to 1 in time t_r and then stays at the constant value of 1.0. Thus,

$$\theta_{,y}(0, t) = 0, \theta_{,y}(1, t) = 0, v(0, t) = 0, \quad (2.8)$$

$$\begin{aligned} v(1, t) &= t/t_r, \quad 0 \leq t \leq t_r, \\ &= 1, \quad t \geq t_r \end{aligned} \quad (2.9)$$

and for dipolar materials, we also assume that

$$\sigma(0, t) = 0, \quad \sigma(1, t) = 0. \quad (2.10)$$

Computations for the domain $-1 \leq y \leq 1$ and with boundary conditions $\sigma(-1, t) = 0$, $\sigma(1, t) = 0$ have given $\sigma(0, t) = 0$.

3. VISCOPLASTIC FLOW RULES

3.1. Litonski's law for nonpolar and dipolar materials

WRIGHT and BATRA (1987) generalized the constitutive relation proposed by LITONSKI (1977) to be applicable to nonpolar and dipolar materials. They assumed that

$$\dot{\gamma}_p = \Lambda s, \quad \dot{d}_p = \frac{\Lambda}{l} \sigma \quad (3.1)$$

and postulated that

$$\Lambda = \max \left[0, \left\{ \left(\frac{s_e}{(1-\alpha\theta) \left(1 + \frac{\psi}{\psi_0} \right)^n} \right)^{1/m} - 1 \right\} / b s_e \right], \quad (3.2)$$

$$s_e = (s^2 + \sigma^2)^{1/2}, \quad (3.3)$$

$$\dot{\psi} = \Lambda s_e^2 / \left(1 + \frac{\psi}{\psi_0} \right)^n. \quad (3.4)$$

Here ψ may be viewed as an internal variable that describes the work hardening of the material. Its evolution is given by (3.4). In (3.2), $(1-\alpha\theta)$ describes the softening of the material due to its heating, b and m characterize its strain-rate hardening, and ψ_0 and n its work hardening. Note that the rate of growth of ψ is proportional to the plastic working. Besides the yield stress in a quasistatic simple shearing test which has been used to non-dimensionalize stress-like quantities, there are five material parameters α , b , m , ψ_0 and n . For dipolar materials, we also need to specify l .

In (3.2)–(3.4) it is implicitly assumed that

$$s_e = (1-\alpha\theta) \left(1 + \frac{\psi}{\psi_0} \right)^n \quad (3.5)$$

describes the loading surface, and if the local state given by $(s, \sigma, \psi, \theta)$ lies inside or on this surface, the plastic strain-rate and the dipolar plastic strain-rate vanish.

3.2. Power law

For nonpolar materials, COSTIN *et al.* (1980) and MARCHAND and DUFFY (1988) have described the dynamic stress–strain curve for steels as

$$s = \left(\frac{\gamma}{\gamma_y} \right)^n \left(\frac{\dot{\gamma}}{\dot{\gamma}_0} \right)^m \left(\frac{\theta}{\theta_0} \right)^v. \quad (3.6)$$

Here γ_y is the strain at yield in a quasistatic simple shear test for which $\dot{\gamma}_0 = 10^{-4} \text{ s}^{-1}$, θ_0 is the reference temperature and θ the current temperature of a material particle in degrees Kelvin. In order to use the power law, we assumed that there is no loading surface and that

$$\dot{\gamma}_p = \dot{\gamma}_0 s^{1/m} \left(\frac{\gamma}{\gamma_y} \right)^{-n/m} \left(\frac{\theta}{\theta_0} \right)^{-v/m}. \quad (3.7)$$

Thus in addition to the yield stress in a quasistatic simple shear test, there are five material parameters $\dot{\gamma}_0$, γ_y , m , n and v .

3.3. Bodner–Partom law

For nonpolar materials undergoing simple shearing deformations, the constitutive relation proposed by BODNER and PARTOM (1975) can be written as

$$\dot{\gamma}_p = D_0 \exp \left[-\frac{1}{2} \left(\frac{K^2}{3s^2} \right)^n \right], \quad n = \frac{a}{\theta} + b, \quad (3.8)$$

$$K = K_1 - (K_1 - K_0) \exp(-mW_p). \quad (3.9)$$

Here θ is the absolute temperature of a material particle, W_p is the plastic work done, and K may be considered as an internal variable. D_0 is the limiting value of the plastic strain-rate and is generally set equal to 10^8 s^{-1} . Besides D_0 , we need to specify a , K_1 , K_0 , m and b to characterize the material. We note that there is no loading or yield surface assumed in this case also.

3.4. Johnson–Cook law

JOHNSON and COOK (1983) tested several materials in simple shear and compression at different strain-rates and found that

$$\dot{\gamma}_p = \exp \left[\left\{ \frac{s}{(A + B\dot{\gamma}_p^n)(1 - T^\alpha)} - 1.0 \right\} / c \right], \quad (3.10)$$

$$T = (\theta - \theta_0) / (\theta_m - \theta_0), \quad (3.11)$$

describe well the test data. Here A , B , n , α , c and θ_m are to be determined experimentally. For θ_m equal to the melting temperature of the material and θ_0 equal to the ambient temperature, they tabulated values of other parameters for several materials. The relation (3.10) is valid for nonpolar materials and presumes that there is no loading surface.

4. CALIBRATION PROCEDURE

4.1. Determination of material parameters

For HY-100 structural steel, MARCHAND and DUFFY (1988) have given the dynamic and quasistatic shear stress–shear strain curves found at strain-rates of 3300 s^{-1} and 10^{-4} s^{-1} respectively. They also reported the values of the exponents m , n and ν for the power law.

In order to calibrate the various flow rules against the same test data we solved, numerically, the initial-boundary value problem outline in Section 2 with

$$\begin{aligned} s(y, 0) &= 1.0, \quad \gamma_p(y, 0) = 0.012, \quad v(y, 0) = y, \quad \theta(y, 0) = 0^\circ\text{C}, \quad \varepsilon = 0, \\ v(1, t) &= 1.0, \quad v(0, t) = 0, \quad \theta_{,y}(0, t) = 0, \quad \theta_{,y}(1, t) = 0, \quad \rho = 7860 \text{ kg/m}^3, \\ c &= 473 \text{ J/kg}^\circ\text{C}, \quad k = 49.73 \text{ W/m}^2\text{C}, \quad H = 2.5 \text{ mm}, \quad \dot{\gamma}_0 = 3300 \text{ s}^{-1}. \end{aligned}$$

Here H is the height of the block and $\dot{\gamma}_0$ is the average applied strain-rate. With no initial temperature perturbation, the block deforms uniformly and homogeneously and the dipolar effects vanish identically. In order to keep to a minimum the number of parameters to be varied, we kept, as far as possible, the values of the strain-hardening exponent and the strain-rate hardening exponent equal to those given by

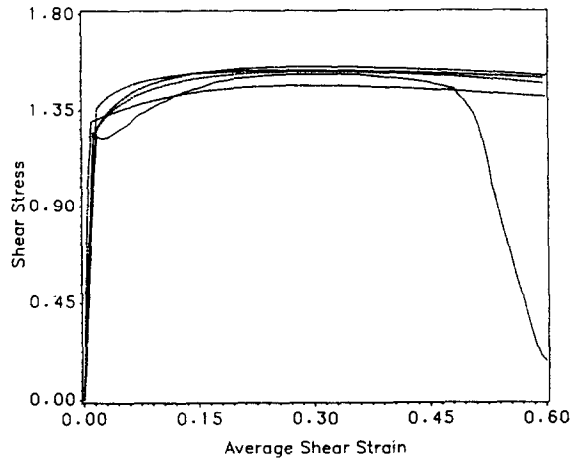


FIG. 1. A comparison of the shear stress–shear strain curves computed by solving an initial-boundary value problem with different flow rules with the experimental stress–strain curve of Marchand and Duffy at a nominal strain-rate of 3300 s^{-1} for a HY-100 structural steel. — experimental, —··— Bodner–Partom, Litonski (non-polar), - - - Litonski (dipolar), — — — — Power, — — — — Johnson–Cook.

MARCHAND and DUFFY (1988), and adjusted the values of parameters describing the thermal softening of the material till the computed stress–strain curve came out close to that given by Marchand and Duffy. For curves depicted in Fig. 1, we used the following values of various material parameters. Note that these curves approximate closely the experimental curve well beyond the value of the nominal strain at which the peak in the stress occurs.

(a) Litonski law for nonpolar and dipolar materials :

$$\alpha = 0.00185/^{\circ}\text{C}, \quad \psi_0 = 0.012, \quad n = 0.107, \quad m = 0.0117, \quad b = 10^4 \text{ s}, \quad l = 0.005.$$

(b) Power law :

$$\dot{\gamma}_0 = 10^{-4} \text{ s}^{-1}, \quad \dot{\gamma}_y = 0.012, \quad \theta_0 = 300\text{K}, \quad m = 0.0117, \quad n = 0.107, \quad v = -0.75.$$

(c) Bodner–Partom law :

$$a = 1200\text{K}, \quad b = 0, \quad K_1 = 3.95, \quad K_0 = 3.21, \quad m = 5.0, \quad D_0 = 10^8 \text{ s}^{-1}.$$

(d) Johnson–Cook law :

$$A = 0.45, \quad B = 1.433, \quad n = 0.107, \quad \theta_m - \theta_0 = 1200^{\circ}\text{C}, \quad \alpha = 0.7, \quad c = 0.0277.$$

We note that the computed curves mimic reasonably well the experimental one till the shear stress begins to drop catastrophically. This rapid drop of the shear stress with increasing shear strain starting with an average strain of 0.50 in the experimental stress–strain curve is due to the initiation and growth of a shear band. We need to simulate a defect in the specimen in order to reproduce this part of the curve.

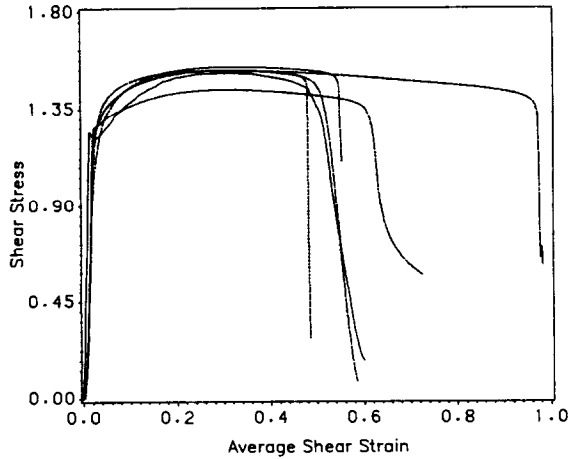


FIG. 2. Shear stress-shear strain curves computed with different flow rules but with the same initial temperature perturbation. See Fig. 1 for the description of various curves.

4.2. Determination of the size of the perturbation

MARCHAND and DUFFY (1988) found that the thickness of their specimens was uniform in the circumferential direction but varied from 5–10% in the axial direction. This and possibly the slight variation in the material properties served as the triggering mechanism for the initiation of a shear band. Here we model the cumulative effect of these inhomogeneities by assuming a nonuniform initial temperature distribution as given by Eq. (2.7). BATRA and LIU (1990) have shown that different ways of modeling a material inhomogeneity give similar results.

Ideally, the same value of ε in (2.7) when used with different flow rules should initiate a shear band, as indicated by the rapid drop of the shear stress, at the value of the nominal strain observed experimentally. Unfortunately, as shown in Fig. 2, for $\varepsilon = 1^\circ\text{C}$, different flow rules predict shear band initiation at widely different values of the nominal strain. No value of ε could be found that will cause the shear band to initiate at the same value of the nominal strain with the different flow rules. We thus have the following two choices. One, to use different values of ε with the various flow rules and the other, to fix ε and find the values of material parameters so as to match the computed stress-strain curves with and without the temperature perturbation with the corresponding experimental ones. This would necessitate changing the values of the strain hardening exponent and/or strain-rate hardening exponent also. This program, though feasible, is very arduous and could be interpreted as manipulating parameters to obtain the desired results. We note in passing that for presumably the same experimental data, HARTLEY *et al.* (1987), KLEPACZKO *et al.* (1987), and MOLINARI and CLIFTON (1987), have given different values of the strain hardening exponent, strain-rate hardening exponent and the thermal softening exponent in the power law. This alludes to the difficulty in obtaining values of various material parameters. Here we adopt the first approach and find ε so that different flow rules

cause the band to initiate at approximately the same value of the nominal strain. This is justifiable because we compare computed results with experimental findings mostly during the growth of the localization process, i.e. post initiation period. Also, we note that the calibration is done at a nominal strain-rate of 3300 s^{-1} , and the comparison of results is made for deformations occurring at nominal strains of 1600 s^{-1} and 1400 s^{-1} . For an assigned value of ε , the initial-boundary value problem outlined in Section 2 with $t_r = 0.033$ was solved by the finite element method. Values of ε equal to 1°C , 2°C , 5°C and 9°C for the Litonski law for nonpolar and dipolar materials, power law, the Bodner–Partom law and the Johnson–Cook law, respectively, result in stress–strain curves shown in Fig. 3. Subsequently, these values of ε for the various flow rules were used.

5. COMPARISON OF NUMERICAL RESULTS WITH EXPERIMENTAL FINDINGS

The curves plotted in Fig. 3 vividly reveal that until the time the shear stress begins to drop rapidly, all of the flow rules considered predict material behavior in reasonable agreement with the experimental observations. For nonpolar materials Litonski's law, the power law and the Johnson–Cook law give essentially a catastrophic drop in the shear stress with virtually no increase in the nominal shear strain. This does not agree with the experimental data since Marchand and Duffy observed that during the drop of the shear stress, the nominal strain increases by approximately 5%. The Litonski law for dipolar materials and the Bodner–Partom law for nonpolar materials do predict the gradual drop in the shear stress in agreement with the experimental data. However, for the Bodner–Partom law the shear stress does not drop as much as it

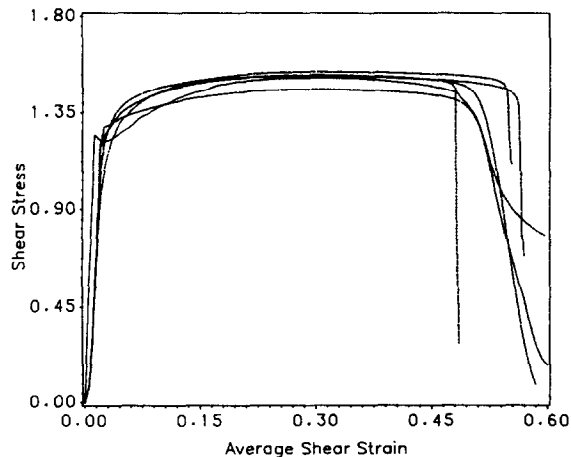


FIG. 3. Shear stress–shear strain curves computed with different flow rules and with different initial temperature perturbation. The objective is to find the size of the initial temperature perturbation in order to initiate a rapid drop of the shear stress at an average strain close to that found experimentally. See Fig. 1 for the description of various curves.

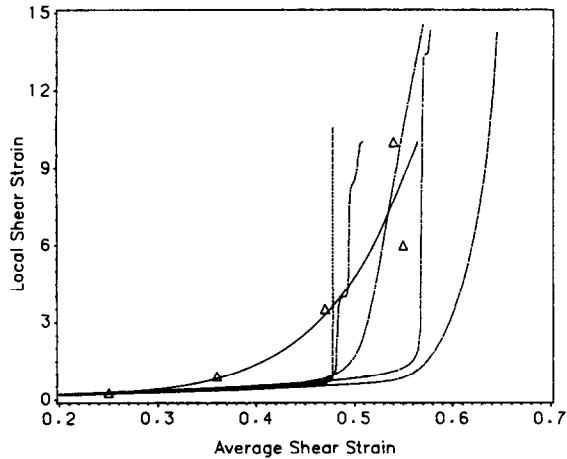


FIG. 4. Growth of the local shear strain within the band as the specimen deforms. See Fig. 1 for the description of various curves. The experimental data points are denoted by a Δ .

does during the tests. The computed value of the shear stress reaches a plateau. Since curves plotted in Fig. 3 were for calibration purposes, these remarks should be regarded as general observations rather than a test of the validity of any of the flow rules.

For a nominal strain-rate of 1600 s^{-1} , Marchand and Duffy have also given values of the shear strain within the band at five different values of the nominal strain. We note that each data point was obtained in a different test and that explains the rather noticeable difference in the values of the local strain within the band for essentially the same value of the nominal strain for the last two data points. These and the corresponding numerically computed results with the different flow rules are plotted in Fig. 4. Whereas the Litonski law, the power law and the Johnson–Cook law give a rapid increase in the local strain once a shear band initiates, the Bodner–Partom law and the Litonski law for dipolar materials give general trends in agreement with the experimental data. We should add that the values of the material parameters and the size of the temperature perturbation were those found earlier and outlined in the preceding section. Also, the computed local strain equals the strain at the center.

With the power law and the Johnson–Cook law, the plastic strain started to oscillate during the time the shear stress was dropping. This was earlier pointed out by BATRA and KIM (1990) and has also been noticed by WRIGHT and WALTER (1989). A possible explanation for this is the interplay between the material hardening due to the strain and strain-rate effects and the thermal softening. This explains the discontinuities in the curves computed with these two flow rules.

The experimental data points plotted in Fig. 5 were taken from the data given in table 4 of Marchand and Duffy's paper. Each data point represents a different test performed at an average strain-rate of approximately 1600 s^{-1} . Since the nominal strain γ_{avg}^* at which the shear stress attained the maximum value s_{max} is different in each test we have plotted in Fig. 5 $\gamma_{\text{avg}}/\gamma_{\text{avg}}^*$ vs s/s_{max} during the time the shear stress is

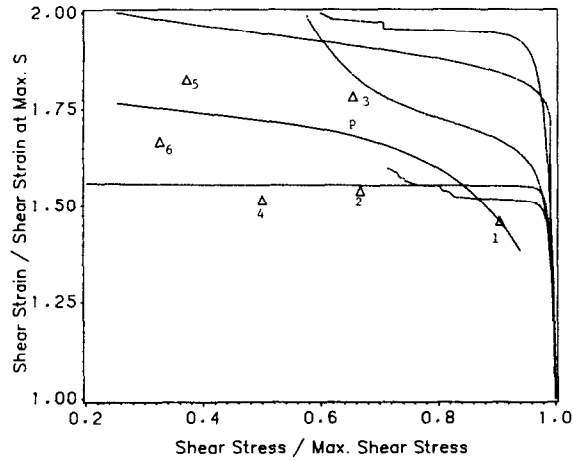


FIG. 5. Plot of normalized shear strain vs the normalized shear stress during the time shear stress is dropping with increasing strain. See Fig. 1 for the description of various curves.

dropping. There is too much scatter in the experimental data to draw any conclusions. Since test points 2 and 3 have abscissa values 0.6667 and 0.6546, we take the midpoint P on the line joining these two points as representing the average of the results for these two tests. If we take the smooth curve passing through the test point 1, point P and the midpoint of the line joining points 5 and 6, we obtain a curve essentially parallel to that computed with the Bodner–Partom law and the Litonski law for dipolar materials. The scarcity of the available experimental data makes a better comparison difficult at this time.

Figures 6–8 depict, respectively, the spatial variation of the plastic strain, the temperature and the flux of linear momentum when $s/s_{\max} = 0.667$ and $\dot{\gamma}_{\text{avg}} = 1600 \text{ s}^{-1}$. We note that the flux of linear momentum equals the shear stress for nonpolar materials and $(s - l\sigma_y)$ for dipolar materials. By the time the momentum flux drops to two-thirds of its maximum value, the shear band should have well developed. In order to highlight the variation of the shear strain, temperature and the shear stress within and near the region of localization of the deformation, we have plotted these quantities on an expanded scale in the region around the shear band center. Both the Johnson–Cook law and the Litonski law for nonpolar materials predict a rather sharp drop in the shear strain at the edges of the band. The Litonski law for dipolar materials gives nearly constant values of the temperature and shear strain within the band. The power law and the Bodner–Partom law give a rather gradual drop of the shear strain and the temperature with the distance from the center of the band. With the dipolar theory the momentum flux takes on the least value at the band center and increases rapidly as we move away from the center and then decreases and stays constant through most of the specimen. The Johnson–Cook law gives a slightly higher value of the shear stress at the center of the band as compared to that at the specimen boundary and the rate of change of the shear stress is constant. With the other flow rules the computed values of the shear stress came out to be essentially constant throughout the specimen.

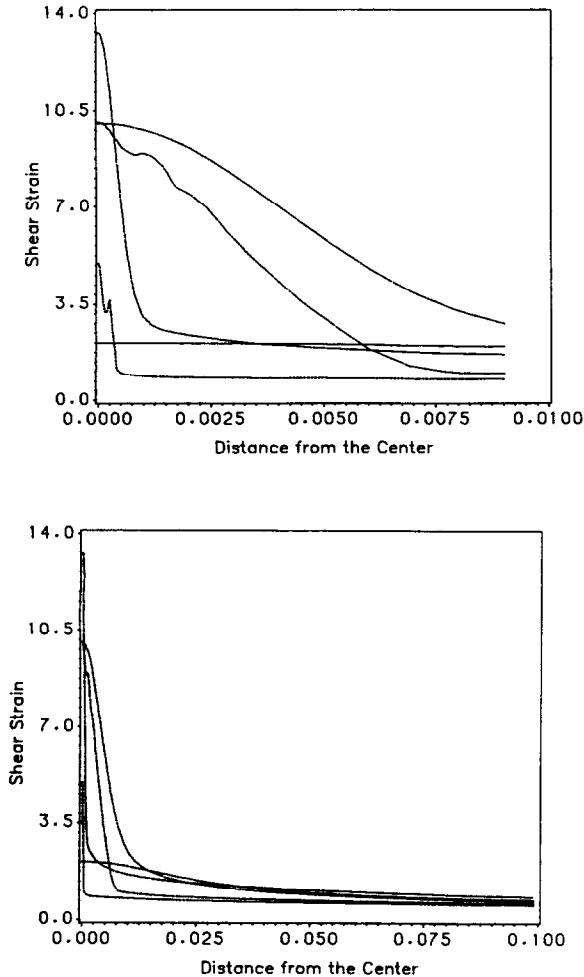


FIG. 6. Spatial variation of the plastic strain when $s/s_{\max} \approx 0.667$. See Fig. 1 for the description of various curves.

Defining the band width as the width of the region over which the plastic shear strain varies by no more than 5% of its value at the center, the computed bandwidth with the Litonski law, the power law, the Bodner-Partom law, the Johnson-Cook law, and the Litonski law for dipolar materials is found to be $2 \mu\text{m}$, $14 \mu\text{m}$, $14 \mu\text{m}$, $6 \mu\text{m}$ and $51 \mu\text{m}$ respectively. For $s/s_{\max} = 0.66$, Marchand and Duffy found the bandwidth to be between $20 \mu\text{m}$ and $55 \mu\text{m}$ depending upon the point of observation around the circumference of the tube. This comparison favors the Bodner-Partom law, the power law and the Litonski law for dipolar materials over the other two flow rules.

In another series of tests on HY-100 steel conducted at a nominal strain-rate of approximately 1400 s^{-1} , Marchand and Duffy measured the temperature within the

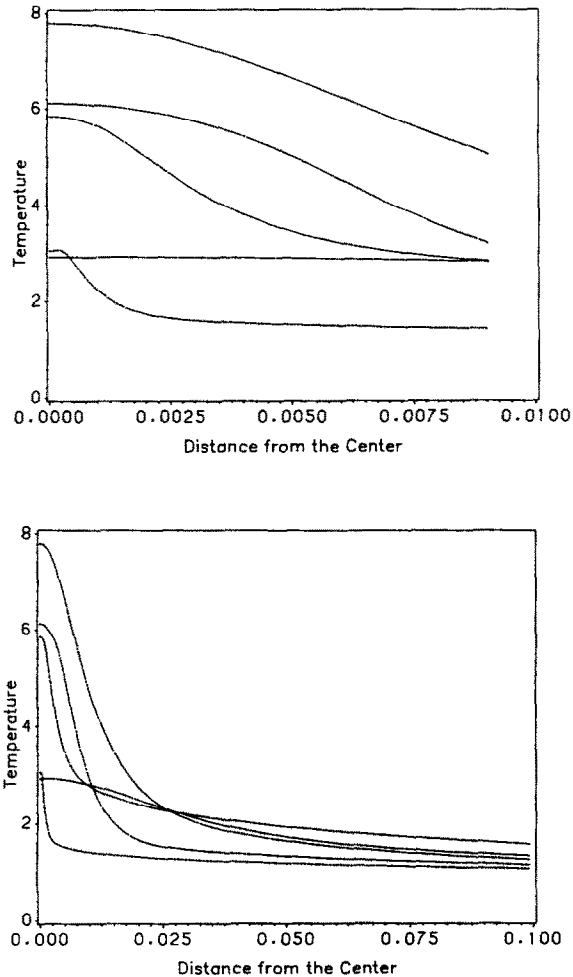


FIG. 7. Spatial variation of the temperature when $s/s_{\max} \approx 0.667$. See Fig. 1 for the description of various curves. The temperature in $^{\circ}\text{C}$ is obtained by multiplying the nondimensional value by 108.9.

band. The data taken from table 5 of their paper is plotted in Fig. 9 along with the computed results for $\dot{\gamma}_{\text{avg}} = 1400 \text{ s}^{-1}$. They measured the temperature over a spot width of $35 \mu\text{m}$ which is larger than the band width. In plotting their data, we have assumed that the reported temperature in the band occurred at the maximum value of the nominal strain in a test. In order to minimize the variation in the results among different tests we have plotted the measured maximum temperature in the band vs $\gamma_{\text{avg}}/\gamma_{\text{avg}}^*$. Even though it is hard to draw a smooth curve through the test data, the detector output plotted in fig. 19 of Marchand and Duffy's paper reveals that the temperature rises during the last stage of the localization process when the shear stress is dropping and that the increase in the average strain during the time temperature rises is about 8%. This observation is in closer agreement with the results computed

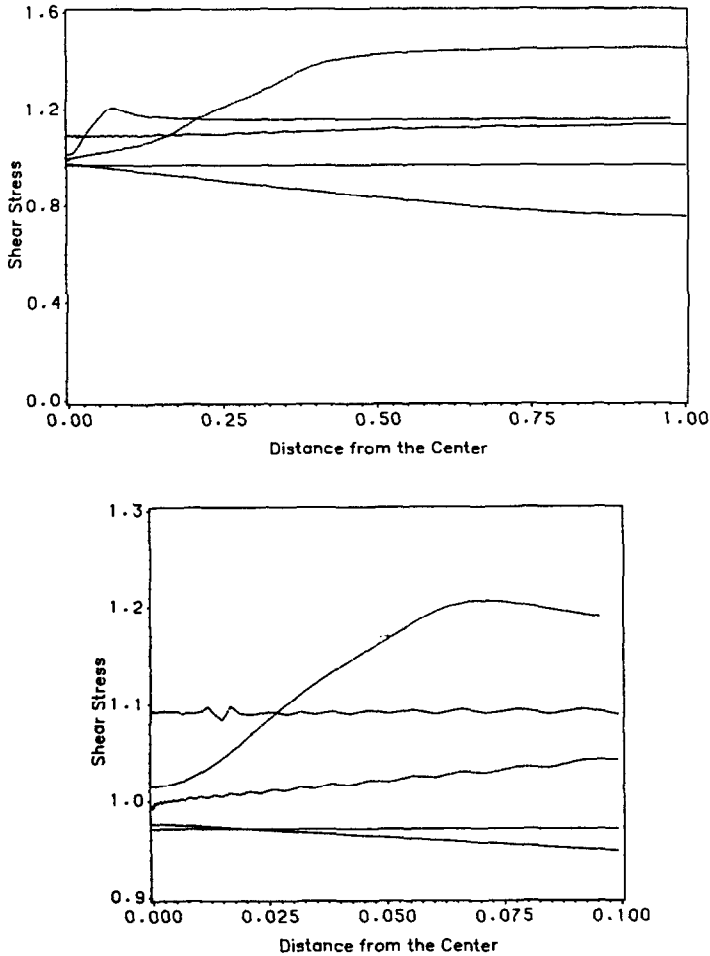


FIG. 8. Spatial description of the flux of linear momentum when $s/s_{max} \approx 0.667$. See Fig. 1 for the description of various curves.

with the Litonski law for dipolar materials. Also, the computed temperature rise of 539°C with this flow rule when $\gamma_{avg}/\gamma_{avg}^* = 1.91$ agrees well with the average value of 475°C found in the eight tests. We should note that the computed temperature within the band of $50\ \mu\text{m}$ width came out to be nearly uniform. Marchand and Duffy estimated that the maximum temperature in the band reached a little over 900°C . Since we do not have any failure criterion included in our work, it is hard to decide when to stop the computations and thus estimate the maximum temperature rise.

Figure 10 shows how the temperature at the center increases after the peak in the shear stress has been attained. It is interesting to note that the temperature, when the shear stress attains the maximum value, is essentially the same for all flow rules. However, the rate of rise of temperature with the drop in the shear stress for the

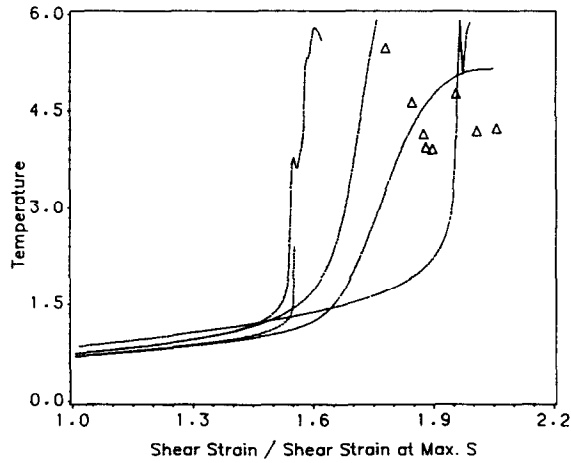


FIG. 9. Temperature at the center vs the normalized shear strain. The experimental data points are denoted by a Δ . See Fig. 1 for the description of various curves.

Johnson–Cook law, the power law and the Bodner–Partom law is nearly the same but differs significantly from that for the Litonski law for nonpolar and dipolar materials. The transition in the slope of the curves near $s/s_{\max} = 1.0$ indicates the point when the rapid drop in the shear stress occurs and the plastic strain rate rises sharply. Thus, the computed temperature rise will depend upon the point when the material is taken to have failed. As pointed out by Marchand and Duffy, once the shear stress begins to collapse, the load carrying capacity of the member is drastically reduced and the material has failed.

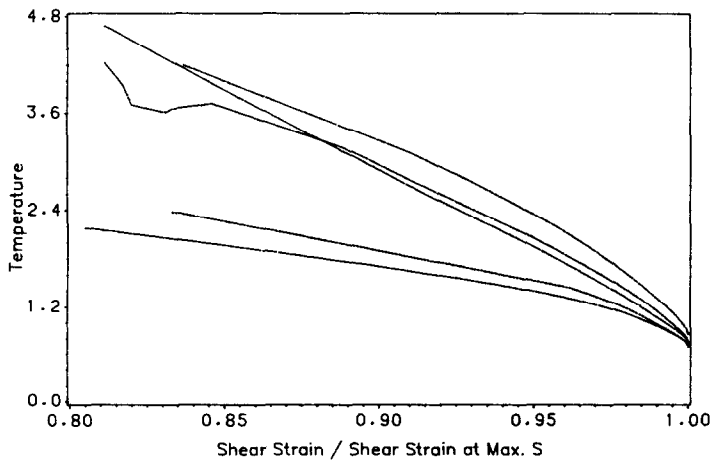


FIG. 10. The evolution of the temperature at the center vs the normalized shear strain during the time the shear stress is dropping. See Fig. 1 for the description of various curves.

6. CONCLUSIONS

We have modeled the dynamic torsional tests of Marchand and Duffy on thin-wall steel tubes by analysing the dynamic deformations of a viscoplastic block undergoing overall simple shearing deformations. A material defect or inhomogeneity has been represented by an initial nonuniform temperature distribution. The focus of the work has been to compare predictions of the various flow rules with the experimental findings during the growth of a shear band. For this purpose, we have also used a dipolar theory and Litonski's flow rule as modified by Wright and Batra and studied extensively by Batra and his coworkers. Whereas it maybe premature to draw definitive conclusions, the Bodner–Partom law and the dipolar theory predict many features of shear banding that are in closer agreement with the experimental observations than the predictions from the power law, the Johnson–Cook law and the Litonski law for nonpolar materials. We note that when finding the values of material parameters for different flow rules, we kept the value of the strain hardening exponent and the strain–rate hardening exponent as close to the test value as possible and varied the parameter describing the thermal softening of the material till the computed stress–strain curve essentially replicated the corresponding experimental curve for nominal strain-rate equal to 3300 s^{-1} . With values of material parameters kept unchanged, computed results for nominal strains equal to 1600 s^{-1} and 1400 s^{-1} were compared with the corresponding experimental findings.

ACKNOWLEDGEMENTS

This work was supported by the U.S. National Science Foundation Grant No. MSM8715952 and the Army Research Office Contract DAAL03-88-K-0184 to the University of Missouri-Rolla. The computations were performed on the IBM 3090-160 vector machine in Columbia, MO under the IBM trial program.

REFERENCES

- | | | |
|--|------|---|
| ANAND, L., LUSH, A. M. and
KIM, K. H. | 1988 | In <i>Thermal Aspects in Manufacturing</i> (edited by M. H. ATTIA and L. KOPS). ASME-PED-Vol. 30, 89. |
| BAI, Y. L. | 1981 | In <i>Shock Waves and High Strain-Rate Phenomenon in Metals</i> , p. 277 (edited by M. A. MYERS and L. E. MURR). Plenum Press, New York. |
| BATRA, R. C. | 1987 | <i>Int. J. Plasticity</i> 3 , 75. |
| BATRA, R. C. and KIM, C. H. | 1990 | <i>Int. J. Plasticity</i> 6 , 127. |
| BATRA, R. C. and LIU, DE-SHIN | 1989 | <i>J. appl. Mech.</i> 56 , 527. |
| BATRA, R. C. and LIU, DE-SHIN | 1990 | <i>Int. J. Plasticity</i> 6 , 231. |
| BODNER, S. R. and PARTOM, Y. | 1975 | <i>J. appl. Mech.</i> 42 , 385. |
| BURNS, T. J. | 1985 | <i>Q. appl. Math.</i> 43 , 65. |
| CLIFTON, R. J. | 1980 | Adiabatic shear in material response to ultrahigh loading rates, U.S. NRC National Material Advisory Board Report NMAB-356 (edited by W. HERRMAN <i>et al.</i>). |
| COLEMAN, B. D. and
HODGDON, M. L. | 1985 | <i>Archs ration. Mech. Anal.</i> 90 , 219. |

- COSTIN, L. S., CRISMAN, E. E., HAWLEY, R. H. and DUFFY, J. 1980 In *Mechanical Properties at High Strain Rates*, p. 90 (edited by J. HARDING). Proc. 2nd Oxford Conf. Inst. Phys., London.
- DILLON, O. W. and KRATOCHVIL, J. 1970 *Int. J. Solids Struct.* **6**, 1513.
- GIOVANOLA, J. 1987 Proc. Impact Loading and Dynamic Behavior of Materials, Bremen, F.R.G.
- HARTLEY, K. A., DUFFY, J. and HAWLEY, R. H. 1987 *J. Mech. Phys. Solids* **35**, 283.
- JOHNSON, G. R. and COOK, W. H. 1983 In *Proc. 7th Int. Symp. Ballistics*, The Hague. The Netherlands, p. 1.
- KLEPACZKO, J. R., LIPINSKI, P. and MOLINARI, A. 1987 In *Proc. Impact Loading and Dynamic Behaviour of Materials*, p. 695 (edited by C. Y. CHIEM, H. D. KUNZE and L. W. MEYER). Informationsgesellschaft, Bremen, F.R.G., 1987.
- LEMONDS, J. and NEEDLEMAN, A. 1986a *Mech. Mater.* **5**, 339.
- LEMONDS, J. and NEEDLEMAN, A. 1986b *Mech. Mater.* **5**, 363.
- LITONSKI, J. 1977 In *Bulletin de l'Académie Polonaise des Sciences, Sciences Tech.*, Vol. 25, 7.
- MARCHAND, A. and DUFFY, J. 1988 *J. Mech. Phys. Solids* **36**, 251.
- MOLINARI, A. and CLIFTON, R. J. 1987 *J. appl. Mech.* **54**, 806.
- MOSS, G. L. 1981 In *Shock Waves and High Strain Rate Phenomenon in Metals*, p. 229 (edited by M. A. MEYERS and L. E. MURR). Plenum Press, New York.
- NEEDLEMAN, A. 1989 *J. appl. Mech.* **56**, 1.
- ROGERS, H. C. 1983 In *Material Behavior Under High Stress and Ultrahigh Loading Rates*, p. 101 (edited by J. MESCALL and V. WEISS). Plenum Press, New York.
- SHAWKI, T. G., CLIFTON, R. J. and MAJDA, G. 1983 Analysis of shear strain localization in thermal visco-plastic materials, Brown Univ. Report, ARO DAAG29-81-K-0121/3.
- TIMOTHY, S. P. 1987 *Acta Metall.* **35**, 301.
- TZAVARAS, A. E. 1987 *Archs ration. Mech. Anal.* **99**, 349.
- WRIGHT, T. W. 1990 *J. Mech. Phys. Solids* **38**, 515.
- WRIGHT, T. W. and BATRA, R. C. 1985 *Int. J. Plasticity* **1**, 205.
- WRIGHT, T. W. and BATRA, R. C. 1987 In *Proc. Macro- and Micro-Mechanics of High Velocity Deformation and fracture*, IUTAM Symp., Tokyo, Aug. 1985, p. 189.
- WRIGHT, T. W. and WALTER, J. W. 1989 Adiabatic shear bands in one-dimension, Ballistic Research Laboratory Report, BRL-MR-3759.
- ZBIB, H. M. and AIFANTIS, E. C. 1988 *Scripta Metall.* **20**, 703.
- ZENER, C. and HOLLOMON, J. H. 1944 *J. appl. Phys.* **15**, 22.